EEG and Path Integral Framework for Spatial-Temporal Neural Summation: the Brain's Neuronal Planck Constant

Dr. Moninder Singh Modgil[1] and Mr. Dhyandeo Dattatray Patil[2]

[1]Cosmos Research Lab, Centre for Ontological Science, Meta Quanta Physics and Omega Singularity email: msmodgil@gmail.com
[2]Electrical and AI Engineering, Cosmos Research Lab email: cosmosresearchlab@gmail.com

September 10, 2025

Abstract

This work develops a unified theoretical framework connecting electroencephalography (EEG), quantum path integrals, and mechanosensitive modulation of neuronal dynamics in meditation. Neurons are modeled as mesoscopic quantum oscillators governed by a brain-specific Planck-like constant, the Brain's Neuronal Planck Constant (h_{Neuron}), estimated to be on the order of 10^{-16} J·s. This formulation allows neuronal firing frequencies to be treated analogously to quantized oscillator states, extending Feynman's path integral formalism to cortical and subcortical ensembles. The framework incorporates mechanosensory contributions from Piezo2 ion channels, which transduce vascular pulsations into periodic perturbations of membrane potentials, thereby entraining cortical and limbic oscillations. EEG rhythms, including sensorimotor rhythm (SMR), occipital alpha, frontal theta, and gamma synchrony, emerge as macroscopic interference fields resulting from coherent sums over neuronal amplitudes. We demonstrate how meditation alters these rhythms by narrowing spectral densities, reducing phase dispersion, and enhancing constructive interference across cortical and deep brain structures such as the thalamus, hippocampus, and amygdala. Predictions include robust SMR and alpha with eyes closed, persistent alpha during eyes-open meditation, theta-gamma coupling in blissful states, and widespread gamma coherence in states of universal love. The integration of EEG, fMRI, and path integral neurodynamics provides a rigorous mesoscopic model linking interoceptive physiology, quantum neurobiology, and meditative phenomenology, offering experimentally testable predictions for the neuroscience of consciousness.

1 Introduction

The study of brain dynamics has traditionally relied upon two parallel methodologies. On the one hand, electroencephalography (EEG) provides a noninvasive window into the collective oscillatory activity of neuronal populations, capturing rhythms such as alpha, beta, theta, and gamma that correlate with distinct cognitive and affective states. On the other hand, theoretical neuroscience has sought mathematical frameworks capable of describing the complexity of neuronal integration across space and time. Th Recent advances suggest that neurons may be conceptualized as mesoscopic quantum oscillators characterized by a Brain's Neuronal Planck Constant (h_{Neuron}), whose estimated value is on the order of 10^{-16} J·s. This constant defines the scale at which neuronal ensembles exhibit quantum-like coherence, enabling a path integral description of brain activity in analogy with quantum mechanics. In this framework, the amplitude associated with a given neuronal trajectory $x(t)$ is expressed as

$$\mathcal{A}[x(t)] = \exp\left(\frac{i}{\hbar_B} S[x(t)]\right), \tag{1}$$

where $S[x(t)]$ is the action functional encoding the dynamics of the neuron and $\hbar_B$ denotes the brain-specific Planck-like constant. The sum over all trajectories leads to a macroscopic field description of cortical rhythms, linking EEG observables with the underlying microscopic dynamics.

An additional regulatory factor is provided by mechanosensitive ion channels, particularly Piezo2, which couple neuronal activity to vascular pulsations. Recent findings have demonstrated that Piezo2 channels transduce fast hemodynamic fluctuations into neuronal signals, establishing a bidirectional link between neuronal path integrals and systemic physiology. This opens the possibility of modeling EEG not solely as a neuronal ensemble phenomenon but as an emergent field shaped by neurovascular coherence.

Meditation provides a unique domain in which these theoretical constructs can be tested. Meditative states are associated with characteristic EEG patterns, including sensorimotor rhythm (SMR) enhancement, occipital alpha modulation, and frontal midline theta emergence. At deeper stages, practitioners report experiences of serenity, bliss, and universal love, which are hypothesized to involve coordinated thalamo-cortical and limbic-prefrontal interactions. The path integral formulation predicts that these The aim of this work is to integrate EEG observations, path integral formulations of neuronal dynamics, and Piezo2-driven vascular modulation into a coherent model of brain function during meditation. By synthesizing experimental evidence from electrophysiology, neuroimaging, and contemplative neuroscience, this paper proposes that EEG rhythms can be rigorously described as emergent macroscopic fields resulting from constructive and destructive interference among neuronal path amplitudes, shaped by bot

2 Calculation of Brain's Neuronal Planck Constant

The total power consumption of the human brain is approximately $P_B \approx 20$ watts. Assuming $N = 10^{11}$ neurons and an average firing frequency $\nu_{\text{Av}} \sim 10^3$ Hz, we define the power

consumed by each neuron as

$$P_i(t) = \frac{E_i(t)}{\Delta t}. \tag{2}$$

With $\Delta t \sim 10^{-3}$ seconds, consistent with the inverse of average firing frequency, the energy per neuron is

$$E_i(t) = h_{\text{Neuron}} \nu_{\text{Av}}. \tag{3}$$

Summing over all neurons, the brain's total power consumption becomes

$$P_B = \sum_{i=1}^{N} P_i(t) = \frac{N h_{\text{Neuron}} \nu_{\text{Av}}}{\Delta t}. \tag{4}$$

Solving for h_{Neuron}, we obtain:

$$h_{\text{Neuron}} = \frac{P_B \Delta t}{N \nu_{\text{Av}}}. \tag{5}$$

Substituting the known values:

$$P_B = 20, \quad \Delta t = 10^{-3}, \quad N = 10^{11}, \quad \nu_{\text{Av}} = 10^3,$$

we find:

$$h_{\text{Neuron}} \approx 10^{-16} \,\text{Joule·second}. \tag{6}$$

This mesoscopic constant is 18 orders of magnitude larger than the conventional Planck constant $h \approx 10^{-34}$ Joule·second, providing a scale-specific quantization suitable for modeling brain functions.

3 Excitation Levels in Brain Regions

Using the formulation in Eq. **??**, we compute the excitation levels n of various brain regions, given their average EEG frequencies ν. Solving for n, we have:

$$n = \frac{E^B}{h_{\text{Neuron}} \nu} - \frac{1}{2}. \tag{7}$$

Substituting values from empirical EEG data, we compute E^B and n for different regions. For example, the limbic system with $\nu = 4$ Hz yields:

$$E^B = h_{\text{Neuron}} \nu = 10^{-16} \times 4 = 4 \times 10^{-16} \text{J}. \tag{8}$$

Using Eq. 7, we get:

$$n = \left(\frac{4 \times 10^{-16}}{10^{-16} \cdot 4} \right) - \frac{1}{2} = 1 - \frac{1}{2} = 0.5. \tag{9}$$

Extending these computations to other regions gives a full excitation map of the brain in terms of mesoscopic quantum levels.

4 Path Integral Formulation of Neuronal Activity

Having established the quantization framework, we now propose a path integral formulation for neuronal energy dynamics. The amplitude for a neuron to transition from state A to B over time interval T is given by the Feynman path integral:

$$\mathcal{A}_{A\to B} = \int \mathcal{D}[x(t)] \exp\left(\frac{i}{\hbar_{\text{Neuron}}} S[x(t)]\right), \tag{10}$$

where $S[x(t)]$ is the action functional over neuronal paths $x(t)$ and $\hbar_{\text{Neuron}} = h_{\text{Neuron}}/2\pi$.

The Lagrangian may be defined phenomenologically as:

$$\mathcal{L}(x, \dot{x}) = \frac{1}{2} m_{\text{eff}} \dot{x}^2 - V(x), \tag{11}$$

where x denotes membrane potential, m_{eff} is an effective neuronal inertia, and $V(x)$ models neurotransmitter-receptor potentials.

Inserting this Lagrangian into Eq. 10 allows the computation of transition amplitudes that take into account multiple neural paths over time. This may be further extended to neural fields by treating x as a field variable $x(\vec{r}, t)$ and rewriting the integral as a functional over space-time paths.

5 Mechanosensitive Modulation of Neural Oscillators via Vascular Pulsation

Recent experimental findings have demonstrated that arterial blood pressure pulsations can directly modulate neuronal excitability in the olfactory bulb, independently of traditional synaptic transmission mechanisms [12]. This observation significantly extends the scope of neuronal input models by introducing a direct mechanical interface between cardiovascular dynamics and neural field activity. The underlying mechanism relies on mechanosensitive ion channels, notably the Piezo2 family, which respond to transient vascular pulsations with rapid changes in conductance and channel opening [13, 14].

To integrate this finding within the framework of the neuronal path integral model, we first extend the quantized neuronal energy equation derived earlier. In the presence of mechanosensory perturbation, the firing frequency $\nu_i(t)$ of a neuron becomes a time-dependent function modulated by periodic pressure pulses. We express this modulation as

$$\nu_i(t) = \nu_0 + \delta\nu_i(t), \tag{12}$$

where ν_0 is the baseline frequency and $\delta\nu_i(t)$ is the fluctuation induced by blood pressure waves.

Empirical evidence from Zhao et al. (2024) supports the existence of such modulations with frequency components corresponding to cardiovascular rhythms, typically in the range of 1–2 Hz in mammals [12]. Modeling $\delta\nu_i(t)$ as a sinusoidal perturbation yields

$$\delta\nu_i(t) = A_i \cos(\omega_{\text{pulse}} t + \phi_i), \tag{13}$$

where A_i is the amplitude of modulation, ω_{pulse} is the pulsation frequency, and ϕ_i is a phase offset unique to each neuron.

Consequently, the quantized neuronal energy becomes

$$E_i^B(t) = \left(n + \frac{1}{2}\right) h_{\text{Neuron}} \left[\nu_0 + A_i \cos(\omega_{\text{pulse}} t + \phi_i)\right], \tag{14}$$

which shows that the energy levels themselves undergo harmonic modulation in synchrony with vascular oscillations.

In the path integral formalism, we define the Lagrangian $\mathcal{L}(x, \dot{x}, t)$ of a neuron incorporating this mechanosensory perturbation as

$$\mathcal{L}(x, \dot{x}, t) = \frac{1}{2} m_{\text{eff}} \dot{x}^2 - V(x) + \gamma x \cos(\omega_{\text{pulse}} t), \tag{15}$$

where γ represents the coupling strength between mechanical stimulus and the neural membrane potential $x(t)$. The corresponding path integral for the transition amplitude from state x_i to x_f becomes

$$\mathcal{A}(x_i \to x_f) = \int \mathcal{D}[x(t)] \exp\left(\frac{i}{\hbar_{\text{Neuron}}} \int_0^T \mathcal{L}(x, \dot{x}, t) dt\right). \tag{16}$$

The additional term $\gamma x \cos(\omega_{\text{pulse}} t)$ in Eq. 15 introduces a periodic driving force into the neuron's dynamical evolution. This is consistent with the experimental observation that mechanosensitive Piezo2 channels convert mechanical stretch into membrane depolarization, thus influencing firing rates. Piezo2 channels are well-known for their fast activation and deactivation kinetics and are distributed densely in olfactory lobe neurons, particularly in the mitral cell layer [14, 13].

Furthermore, simulations and pharmacological interventions presented in [12] indicate that the removal of vascular pressure pulsations results in the disappearance of slow oscillatory local field potentials (LFPs). This supports the physical validity of modeling $\delta\nu_i(t)$ as a periodic, mechanosensory-driven term. Hence, our path integral formulation accommodates a new class of perturbations that arise not from cognitive or synaptic stimuli but from systemic physiological signals.

This opens the possibility of redefining interoceptive awareness in terms of path integrals over fields modulated by internal bodily signals. In this sense, the brain is not only a receiver of external sensory inputs but also a quantum-mechanical observer of internal rhythms, a view supported by foundational ideas in quantum neurobiology as articulated by Eccles and Wigner [19, 16].

6 Bohmian Neurodynamics, Quantum Potential, and Path Integrals in Mechanosensitive Neural Systems

In this section, we integrate three theoretical frameworks: the path integral formulation of neural dynamics, the Bohmian interpretation of quantum mechanics applied to neuronal

firing, and recent findings on mechanosensitive modulation via Piezo2 channels. The synthesis of these concepts leads to a coherent model of neural activity where the neuron's membrane potential evolves under the influence of a quantum potential, periodic mechanical modulations, and classical electrophysiological fields.

The Bohmian model introduces a hidden-variable theory where the dynamics of a physical system are governed not only by classical potentials but also by an additional term known as the quantum potential. In the context of neuronal modeling, the membrane voltage $x(t)$ can be treated as a Bohmian trajectory guided by a quantum potential $Q(x,t)$. The total wavefunction $\Psi(x,t)$ associated with the neuron's state is expressed in polar form as

$$\Psi(x,t) = R(x,t)e^{iS(x,t)/\hbar}, \tag{17}$$

where $R(x,t)$ is the real-valued amplitude and $S(x,t)$ is the phase. Substituting Eq. 17 into the Schrödinger equation and separating real and imaginary parts leads to the definition of the quantum potential:

$$Q(x,t) = -\frac{\hbar^2}{2m}\frac{1}{R(x,t)}\frac{\partial^2 R(x,t)}{\partial x^2}. \tag{18}$$

The neuronal membrane trajectory then evolves according to the modified Newtonian equation:

$$m\frac{d^2x}{dt^2} = -\frac{dV(x)}{dx} - \frac{dQ(x,t)}{dx}, \tag{19}$$

where $V(x)$ represents the classical membrane potential function determined by ionic gradients and channel dynamics. This approach has been developed extensively in the context of quantum foundations by Bohm and Hiley, and its application to neurodynamics has been proposed by Modgil [20].

When combined with the influence of mechanosensitive channels such as Piezo2, as observed in Zhao et al. [12], the membrane potential $x(t)$ acquires an additional time-dependent modulation due to vascular pulsation. The experimental findings suggest that Piezo2 activation leads to oscillatory field potentials in the mitral cell layer, which persist even in the absence of synaptic input. This effect can be modeled as a periodic external force in the Lagrangian:

$$\mathcal{L}(x,\dot{x},t) = \frac{1}{2}m\dot{x}^2 - V(x) - Q(x,t) + \gamma x\cos(\omega_{\text{pulse}}t), \tag{20}$$

where γ quantifies the coupling strength between mechanical pressure and membrane displacement, and ω_{pulse} is the angular frequency of arterial pulsation.

The corresponding path integral formulation of the transition amplitude from state x_i to x_f over a time interval T is then given by

$$\mathcal{A}(x_i \to x_f) = \int \mathcal{D}[x(t)] \exp\left(\frac{i}{\hbar_{\text{Neuron}}}\int_0^T \mathcal{L}(x,\dot{x},t)dt\right), \tag{21}$$

where $\hbar_{\text{Neuron}}$ is the mesoscopic Planck constant defined in earlier sections, and $\mathcal{L}(x,\dot{x},t)$ is specified by Eq. 20. This integral accounts for all possible paths of the membrane voltage, each weighted by the classical, quantum, and mechanosensitive action contributions.

The advantage of combining the Bohmian and path-integral approaches lies in their complementary interpretations. While the path integral formalism emphasizes the probabilistic

summation over histories, the Bohmian approach identifies a unique trajectory determined by both classical and quantum potentials. In the presence of Piezo2-based periodic driving, both models predict that the neural system exhibits coherent oscillations entrained to the external vascular rhythm. This coherence is experimentally observable Furthermore, the role of the quantum potential is not merely mathematical but introduces a form of nonlocality and contextuality to the neuronal dynamics. In Bohmian theory, the quantum potential arises from the form of the wavefunction and hence is sensitive to the configuration of the entire neural network. This supports the view that consciousness and perception may emerge from nonlocal field configurations rather than localized neuronal firings, an idea that has been advocated by Wigner and Eccles

.

7 Mechanosensitive Modulation of Cortical Field Dynamics via Piezo2 and Neuronal Path Integrals with $\hbar_B$

In the mesoscopic formulation of neural quantum dynamics, neurons are treated as quantum mechanical oscillators with dynamics governed by a brain-specific Planck-like constant $\hbar_B$. The configuration of neural activity across a cortical region is described by a field $\phi(x,t)$, where $x \in R^2$ spans the retinotopic or somatotopic coordinate space, and t denotes perceptual time. The quantum amplitude associated with the neural evolution of this field is computed via a Feynman path integral over all possible field configurations:

$$\mathcal{Z}_{\text{cortex}} = \int \mathcal{D}[\phi(x,t)] \exp\left(\frac{i}{\hbar_B} S[\phi]\right), \tag{22}$$

where $S[\phi]$ is the cognitive action functional defined over the cortical domain and $\hbar_B$ is a mesoscopic constant tailored to the scale of neuronal excitations.

The corresponding Lagrangian density $\mathcal{L}$ governing the local dynamics of $\phi(x,t)$ was introduced as

$$\mathcal{L} = \frac{1}{2}(\partial_t \phi)^2 - \frac{v^2}{2}(\nabla \phi)^2 - V(\phi), \tag{23}$$

where v is the characteristic signal velocity across the cortical substrate, and $V(\phi)$ encapsulates local potential energies associated with excitation, inhibition, or resonance. In the absence of external mechanical modulation, this model provides a field-theoretic representation of perceptual dynamics.

Recent experimental findings by Zhao et al. [12] have demonstrated that Piezo2 mechanosensitive ion channels, located in mitral cells and other olfactory bulb neurons, transduce arterial pressure pulsations into cortical oscillations. The neural oscillations thus generated are phase-locked to cardiovascular rhythms and persist in the absence of cortical synaptic input. This suggests that the cortical Lagrangian should include an explicit coupling term to external periodic pressure stimuli.

To incorporate these effects, we augment the Lagrangian density $\mathcal{L}$ with a time-dependent driving term:

$$\mathcal{L}_{\text{total}} = \frac{1}{2}(\partial_t \phi)^2 - \frac{v^2}{2}(\nabla \phi)^2 - V(\phi) + \eta \phi(x,t)\cos(\omega_{\text{pulse}} t), \tag{24}$$

where η denotes the coupling strength of mechanosensory input, and ω_{pulse} is the angular frequency of the arterial pulse. This term models the periodic depolarization induced by Piezo2 transduction of mechanical stress into ionic currents.

The total quantum amplitude for cortical evolution, now accounting for mechanosensitive perturbations, becomes:

$$\mathcal{Z}_{\text{Piezo2}} = \int \mathcal{D}[\phi(x,t)] \exp\left(\frac{i}{\hbar_B}\int dt\, d^2x \left[\mathcal{L} + \eta \phi(x,t)\cos(\omega_{\text{pulse}} t)\right]\right). \tag{25}$$

This modified path integral reveals how cortical wavefunctions can become entrained by internal bodily rhythms, a phenomenon likely contributing to interoceptive awareness. Since $\hbar_B$ operates at mesoscopic energy scales, on the order of $\sim 10^{-16}$ J·s as estimated in previous work, the path integral is finely tuned to perceptual-level fluctuations.

Mechanistically, Piezo2 ion channels generate transmembrane depolarizations through conformational gating under mechanical stress. These channels are fast-acting, non-selective cation pathways that directly link changes in blood pressure to neuronal firing rates. Zhao et al. [12] showed that in isolated olfactory bulb preparations, stimulation by pulsatile mechanical pressure produces low-frequency field oscillations that mirror cardiovascular dynamics. In this model, the coupling constant η can be empiricall Further, interference patterns between mechanically driven oscillations and endogenous cortical wavefunctions lead to phase synchronization phenomena, which may be computed through saddle-point approximations of the path integral. These interference terms, emerging from the action functional $S[\phi]$, depend on both intrinsic cortical geometry and extrinsic pulse phase, offering a plausible substrate for perceptual binding.

To conclude, the incorporation of Piezo2-mediated mechanotransduction into the path integral formulation of the quantum brain provides a rigorous foundation for understanding the entrainment of perception and consciousness to systemic physiological rhythms. It unifies vascular interoception with cortical field evolution in a field-theoretic framework governed by $\hbar_B$.

8 Electroencephalography as a Coherent Sum over Neuronal Path Integrals

In the mesoscopic quantum model of the brain, each neuron is modeled as a quantum mechanical oscillator whose dynamics contribute a complex-valued amplitude to the overall cortical field configuration. These amplitudes evolve according to individual Lagrangians and are integrated over all possible paths using a brain-specific Planck constant $\hbar_B$. The macroscopic electroencephalogram (EEG) signal observed on the scalp or cortex is thus interpreted as an emergent interference pattern, arising from the Let the action $S_i[x(t)]$ describe

the evolution of the i^{th} neuron's membrane potential $x_i(t)$, subject to a local Lagrangian $\mathcal{L}_i(x_i, \dot{x}_i, t)$:

$$S_i = \int_0^T \mathcal{L}_i(x_i, \dot{x}_i, t)\, dt. \tag{26}$$

Each neuron contributes a complex amplitude to the field:

$$\mathcal{A}_i = \int \mathcal{D}[x_i(t)] \exp\left(\frac{i}{\hbar_B} S_i[x_i(t)]\right), \tag{27}$$

which may be interpreted as a quantum mechanical propagator in cortical configuration space.

The EEG signal at a spatial location x and time t is defined as the real part of the coherent sum over all neuronal amplitudes in a cortical volume Ω:

$$\Phi(x,t) = \Re\left\{\sum_{i\in\Omega} \mathcal{A}_i(t)\right\}. \tag{28}$$

This formulation emphasizes that $\Phi(x,t)$ is not merely the sum of firing rates or spike counts, but the interference sum over the complex-valued transition amplitudes of all neurons in a given region. In regions of high phase coherence between neurons, constructive interference amplifies $\Phi(x,t)$, generating rhythmic EEG waves. Conversely, phase dispersion leads to destructive interference and signal quenching.

Furthermore, frequency components of the EEG can be traced to dominant phase differences in $\mathcal{A}_i(t)$. If a subgroup of neurons oscillates with synchronized phase $\theta(t)$ and fundamental frequency ω, then:

$$\mathcal{A}_i(t) \sim A_i \exp\left(\frac{i}{\hbar_B} E_i t\right) = A_i \exp(i\omega t), \tag{29}$$

leading to an aggregate EEG contribution:

$$\Phi(x,t) \sim \sum_i A_i \cos(\omega t + \phi_i), \tag{30}$$

where ϕ_i encodes initial phase differences. This summation yields band-limited oscillatory components characteristic of EEG rhythms: delta (< 4 Hz), theta (4–7 Hz), alpha (8–12 Hz), beta (13–30 Hz), and gamma (> 30 Hz).

The spectral density of $\Phi(x,t)$ is thus determined by the distribution of energy levels E_i and their corresponding synchrony within the cortical ensemble. This allows us to interpret EEG power fluctuations as emergent quantum interference phenomena mediated by path integrals over neuronal membrane potentials.

Incorporating Piezo2-modulated Lagrangians from Section 5, the individual $\mathcal{L}_i$ acquire periodic driving terms of the form:

$$\mathcal{L}_i \to \mathcal{L}_i + \gamma_i x_i(t) \cos(\omega_{\text{pulse}} t), \tag{31}$$

which entrain $\mathcal{A}_i(t)$ to vascular rhythm. This modulation causes low-frequency synchronization of neuronal phases across the cortex, reflected as increased EEG coherence in low-frequency bands, in line with Zhao et al. [12].

This field-theoretic model unifies classical EEG phenomenology with quantum amplitude dynamics, and offers a formal basis for understanding how interoceptive physiological rhythms (e.g., heartbeat) may entrain perception and cognition through neuronal synchrony observable in EEG recordings.

9 Sensorimotor Rhythm (SMR) as Emergent Coherence from Neuronal Path Integrals

To illustrate the preceding theory, we now consider the emergence of the sensorimotor rhythm (SMR), a prominent EEG component observed in the 12–15 Hz range over sensorimotor cortex. SMR is typically associated with states of physical stillness and focused attention, and is modulated by volitional and interoceptive cues. Within the framework of quantum neural dynamics, SMR arises as a mesoscopic interference phenomenon resulting from partial synchrony across populations of cortical neurons in motor- Let us assume that in a sensorimotor cortical region Ω_{SMR}, the neuronal Lagrangians are perturbed by low-amplitude proprioceptive and interoceptive inputs, modeled via modulated potentials $V_i(x_i, t)$. These perturbations entrain a subset of neurons into a shared oscillatory mode with angular frequency $\omega_{\text{SMR}} \approx 2\pi \cdot 13.5$ rad/s.

Each neuron's amplitude, in this resonant subpopulation, becomes phase-locked:

$$\mathcal{A}_i(t) \approx A_i \exp(i\omega_{\text{SMR}} t + \phi_i), \tag{32}$$

where A_i and ϕ_i are neuron-specific amplitude and phase. The SMR field is given by:

$$\Phi_{\text{SMR}}(x, t) = \Re \left\{ \sum_{i \in \Omega_{\text{SMR}}} A_i \exp(i\omega_{\text{SMR}} t + \phi_i) \right\}. \tag{33}$$

Under moderate phase coherence, we approximate:

$$\Phi_{\text{SMR}}(x, t) \approx \bar{A}(x) \cos(\omega_{\text{SMR}} t + \bar{\phi}(x)), \tag{34}$$

where $\bar{A}(x)$ and $\bar{\phi}(x)$ represent the spatially averaged amplitude and phase in region Ω_{SMR}.

The emergence of SMR from this sum is consistent with the concept of a **macroscopic order parameter** in quantum field theory, where many-body coherence produces measurable classical fields. Here, $\Phi_{\text{SMR}}(x, t)$ serves as the EEG-visible manifestation of synchronized sub-threshold membrane oscillations in the $\sim$13 Hz range. Importantly, this rhythm arises from **non-firing** fluctuations and thus reflects global field alignment rather than spiking synchrony alone.

Incorporating Piezo2-driven vascular entrainment, the Lagrangian density for each neuron includes:

$$\mathcal{L}_i(t) \to \mathcal{L}_i(t) + \gamma_i x_i(t) \cos(\omega_{\text{pulse}} t), \tag{35}$$

where $\omega_{\text{pulse}} \approx 1$–$2$ Hz. This slow modulation can facilitate SMR coherence via frequency locking and cross-frequency coupling, especially in quiet, interoceptively aware states.

These theoretical predictions align with empirical findings in EEG neurofeedback studies, where voluntary enhancement of SMR is associated with relaxed alertness, improved motor control, and reduced somatic reactivity. Such modulations, in our framework, reflect dynamic tuning of the quantum phase landscape across neuronal populations in sensorimotor cortex.

10 Occipital Cortex, Alpha Rhythm, and the Difference Between Closed and Open Eyes

The occipital cortex, particularly the visual Brodmann areas 17, 18, and 19, exhibits one of the most robust demonstrations of macroscopic neural coherence in electroencephalography (EEG). With eyes closed, the primary and associative visual cortices produce pronounced alpha oscillations in the range of 8–12 Hz. Upon opening the eyes, these oscillations undergo suppression or desynchronization, a phenomenon first described by Hans Berger in 1929 [26] and further analyzed in the context of neu Within the path integral model of brain dynamics, this difference can be represented by the degree of phase coherence across neuronal oscillators in the occipital cortex. Let $\phi(x,t)$ represent the cortical field configuration at retinotopic coordinate x and perceptual time t. The quantum amplitude of visual cortex evolution is then expressed as

$$\mathcal{Z}_{\text{V1-V3}} = \int \mathcal{D}[\phi(x,t)] \exp\left(\frac{i}{\hbar_B} S[\phi]\right), \tag{36}$$

where $\hbar_B$ is the brain-specific Planck-like constant and $S[\phi]$ is the cognitive action functional across Brodmann areas 17 (V1), 18 (V2), and 19 (V3).

The cognitive Lagrangian density can be written as

$$\mathcal{L}(\phi, \partial_t\phi, \nabla\phi) = \frac{1}{2}(\partial_t\phi)^2 - \frac{v^2}{2}(\nabla\phi)^2 - V(\phi), \tag{37}$$

where v is the characteristic propagation velocity across the cortical surface, and $V(\phi)$ encodes excitatory-inhibitory balance. During eyes-closed conditions, the excitatory drive from external input is minimal, leading to dominance of intrinsic oscillatory modes. These modes synchronize across populations of neurons, yielding constructive interference in the summation of amplitudes.

The EEG potential recorded at occipital electrodes is the real part of the summed neuronal amplitudes across the visual field representation:

$$\Phi_{\text{EEG}}(t) = \Re\left\{\sum_{i \in \Omega_{\text{occipital}}} \mathcal{A}_i(t)\right\}, \tag{38}$$

where each $\mathcal{A}_i(t)$ is defined by

$$\mathcal{A}_i(t) = \int \mathcal{D}[x_i(t)] \exp\left(\frac{i}{\hbar_B}\int_0^T \mathcal{L}_i(x_i, \dot{x}_i, t)dt\right). \tag{39}$$

For eyes-closed conditions, the oscillatory frequency ω_α emerges as the dominant collective mode, with individual amplitudes approximated by

$$\mathcal{A}_i(t) \sim A_i \exp(i\omega_\alpha t + \phi_i), \tag{40}$$

where $\omega_\alpha \approx 2\pi \times 10$ rad/s. Phase coherence across the ensemble yields a macroscopic field

$$\Phi_{\text{alpha}}(t) \approx \bar{A} \cos(\omega_\alpha t + \bar{\phi}), \tag{41}$$

which corresponds to the classical EEG alpha rhythm.

When the eyes are open, visual input drives neurons in V1, V2, and V3 into multiple asynchronous modes. Let the frequency distribution of neuronal oscillations be given by a spectral density function $\rho(\omega)$. Then the EEG field is approximated by

$$\Phi_{\text{open}}(t) \approx \int d\omega\, \rho(\omega) \cos(\omega t + \phi(\omega)), \tag{42}$$

which, due to phase dispersion, has reduced amplitude in the alpha band. This phenomenon corresponds to alpha desynchronization or event-related desynchronization (ERD) [27].

The difference between closed and open eyes thus arises from interference principles inherent to the path integral formulation. With eyes closed, narrow-band synchronization yields constructive interference and high-amplitude alpha. With eyes open, broad-band dispersion leads to destructive interference and reduced alpha amplitude. Brodmann area 17, being the primary retinotopic map, shows the strongest modulation, while associative areas 18 and 19 contribute to the rapid suppression of coherence under vi This theoretical account aligns with neurophysiological evidence showing that alpha oscillations serve as an idling rhythm in visual cortex [28], representing a state of readiness that is disrupted when external visual input necessitates processing. Within the path integral framework, the eyes-open transition can be described as a broadening of the action landscape $S[\phi]$, leading to greater diversity of trajectories in the functional integral and reduced coherence in the summed amplitu

11 Predictions for Sensorimotor Rhythm and Occipital Cortex Alpha in Meditative States

Meditative states offer a unique context in which to test predictions derived from the path integral model of cortical dynamics. By combining the analysis of sensorimotor rhythm (SMR) in Brodmann areas of motor cortex with occipital alpha oscillations in Brodmann areas 17, 18, and 19, one can establish clear expectations regarding EEG patterns during body stillness and different visual conditions. The theoretical framework developed in earlier sections, which treats neurons as mesoscopic oscillators with

$$\mathcal{Z} = \int \mathcal{D}[\phi(x,t)] \exp\left(\frac{i}{\hbar_B} S[\phi]\right), \tag{43}$$

with $S[\phi]$ the cognitive action functional, is particularly well suited for describing the phase coherence properties underlying EEG rhythms in meditation.

When the body is still and the eyes are closed, motor cortex receives minimal proprioceptive feedback, while visual cortex receives no external sensory input. In this scenario, neuronal oscillators are dominated by intrinsic dynamics, producing constructive interference in their summed path amplitudes. Let the SMR frequency be $\omega_{\text{SMR}} \approx 2\pi \times 13.5$ rad/s. The amplitude of a single neuronal oscillator contributing to SMR is given by

$$\mathcal{A}_i^{\text{SMR}}(t) \sim A_i \exp(i\omega_{\text{SMR}} t + \phi_i), \tag{44}$$

and the macroscopic SMR field is expressed as

$$\Phi_{\text{SMR}}(t) = \Re \left\{ \sum_{i \in \Omega_{\text{SMR}}} \mathcal{A}_i^{\text{SMR}}(t) \right\}. \tag{45}$$

In meditative stillness with eyes closed, the phase dispersion among neurons in Ω_{SMR} is minimized, yielding

$$\Phi_{\text{SMR}}(t) \approx \bar{A} \cos(\omega_{\text{SMR}} t + \bar{\phi}), \tag{46}$$

where $\bar{A}$ is the average amplitude and $\bar{\phi}$ the average phase. This predicts robust SMR activity, consistent with empirical studies showing increased SMR during states of relaxed alertness [29].

At the same time, in the occipital cortex, with eyes closed, alpha oscillations dominate. Each neuron contributes an amplitude at $\omega_\alpha \approx 2\pi \times 10$ rad/s,

$$\mathcal{A}_j^{\alpha}(t) \sim B_j \exp(i\omega_\alpha t + \theta_j), \tag{47}$$

so that the macroscopic field becomes

$$\Phi_\alpha(t) = \Re \left\{ \sum_{j \in \Omega_{\text{V1-V3}}} \mathcal{A}_j^{\alpha}(t) \right\}. \tag{48}$$

In eyes-closed meditation, $\Phi_\alpha(t)$ has high amplitude due to narrow-band coherence, corresponding to the classical alpha rhythm originally described by Berger [26]. The path integral formulation interprets this as a narrowing of the spectral density $\rho(\omega)$ of neuronal oscillators, yielding constructive interference at ω_α and stable alpha oscillations in V1, V2, and V3.

When the body is still and the eyes are open, motor cortex remains in a state of minimal movement, preserving partial SMR coherence. However, visual cortex receives continuous input. Under normal waking conditions, this broadens the distribution $\rho(\omega)$ across V1, V2, and V3, leading to alpha desynchronization as described by Pfurtscheller and Lopes da Silva [27]. In meditation with eyes open, however, attentional regulation suppresses the processing of external input. The actio

$$\Phi_{\text{open, occipital}}(t) \approx \int d\omega\, \rho_{\text{med}}(\omega) \cos(\omega t + \theta(\omega)), \tag{49}$$

where $\rho_{\text{med}}(\omega)$ is narrower than the distribution in ordinary eyes-open states. As a result, alpha activity persists even with open eyes, a phenomenon reported in studies of advanced meditation practitioners [30].

Similarly, SMR in the eyes-open meditative state is modeled as

$$\Phi_{\text{SMR, open}}(t) = \Re\left\{\sum_{i\in\Omega_{\text{SMR}}} A_i \exp(i\omega_{\text{SMR}}t + \phi_i)\right\}, \tag{50}$$

with moderate coherence levels. The predicted outcome is maintenance of SMR power due to suppression of extraneous proprioceptive and motor pathways, combined with partial entrainment by Piezo2-modulated low-frequency rhythms as described in Zhao et al. [12]. This suggests enhanced cross-frequency coupling between SMR and slower interoceptive rhythms such as heartbeat and respiration.

In summary, the path integral model predicts that meditation with eyes closed leads to strong SMR and alpha coherence, reflecting constructive interference across neuronal ensembles. Meditation with eyes open, in contrast, attenuates the expected alpha desynchronization by narrowing the spectral density of neuronal oscillations, thereby allowing alpha coherence to persist despite visual inflow. These predictions align with empirical findings in contemplative neuroscience, which report enhanced occipital a

12 Auditory Cortex, Meditation, and the Role of Music in Path Integral Neurodynamics

The auditory cortex, encompassing Brodmann areas 41 and 42 in the primary auditory region and area 22 in the superior temporal gyrus, provides a compelling site to analyze the interplay between external sensory input and intrinsic neuronal dynamics during meditation. Within the framework of path integral neurodynamics, neuronal ensembles in these regions are modeled as oscillatory systems whose amplitudes evolve according to the cognitive action functional $S[\phi]$, mediated by the mesoscopic Planck con

$$\mathcal{Z}_{\text{auditory}} = \int \mathcal{D}[\phi(x,t)] \exp\left(\frac{i}{\hbar_B} S[\phi]\right), \tag{51}$$

where $\phi(x,t)$ encodes the field configuration across auditory cortex and $\hbar_B$ sets the mesoscopic quantum scale of neural oscillations [20].

When the body is still and the eyes are closed, auditory neurons are relatively free from competing visual or proprioceptive interference. If no music is present, the oscillations in auditory cortex manifest as idling rhythms in the alpha and low beta range, arising primarily from intrinsic excitatory-inhibitory cycles. The amplitude of a single neuron in such conditions may be represented as

$$\mathcal{A}_i^{\text{idle}}(t) \sim C_i \exp(i\omega_{\text{idle}}t + \psi_i), \tag{52}$$

with $\omega_{\text{idle}} \in [2\pi\cdot 8, 2\pi\cdot 20]$ rad/s corresponding to 8–20 Hz activity. The macroscopic auditory field is then

$$\Phi_{\text{idle}}(t) = \Re\left\{\sum_{i\in\Omega_{\text{auditory}}} \mathcal{A}_i^{\text{idle}}(t)\right\}, \tag{53}$$

which yields low-amplitude, unsynchronized oscillations consistent with auditory cortex resting state [28].

When music is introduced during meditation with eyes closed, the auditory cortex is entrained by rhythmic and harmonic structures of the stimulus. Let ω_{music} denote the fundamental angular frequency of a rhythmic beat, often in the delta or theta range, and ω_{endog} the intrinsic oscillatory frequency of the neuronal ensemble. The resulting neuronal amplitude is then expressed as

$$\mathcal{A}_i^{\text{music}}(t) \sim D_i \exp\left(i(\omega_{\text{endog}} + \omega_{\text{music}})t + \chi_i\right), \tag{54}$$

which incorporates a frequency shift corresponding to cross-frequency coupling between intrinsic and stimulus-driven oscillations. The total macroscopic field becomes

$$\Phi_{\text{music, closed}}(t) = \Re\left\{ \sum_{i \in \Omega_{\text{auditory}}} D_i \exp\left(i(\omega_{\text{endog}} + \omega_{\text{music}})t + \chi_i\right) \right\}, \tag{55}$$

indicating entrainment of cortical ensembles to the external rhythmic structure. Empirical work supports this prediction, showing enhanced theta and gamma coherence in auditory cortex during music perception and meditation [31].

In contrast, when the body is still and the eyes are open without music, auditory cortex displays baseline idling rhythms as in Eq. 52, but occipital cortex simultaneously undergoes alpha desynchronization due to visual input. This creates a cross-modal state where auditory idling oscillations coexist with reduced visual coherence. The spectral density function $\rho(\omega)$ of auditory oscillators remains broad, preventing the emergence of strong phase locking. The EEG field is then

$$\Phi_{\text{open, no music}}(t) \approx \int d\omega\, \rho(\omega) \cos(\omega t + \psi(\omega)), \tag{56}$$

with reduced overall amplitude compared to eyes-closed conditions.

When meditation is practiced with body still and eyes open while listening to music, however, the situation changes significantly. Auditory cortex remains entrained to rhythmic inputs, and the coherence induced by music counteracts the dispersive influence of visual input. The field amplitude in this condition is given by

$$\Phi_{\text{music, open}}(t) = \Re\left\{ \sum_{i \in \Omega_{\text{auditory}}} D_i \exp\left(i(\omega_{\text{endog}} + \omega_{\text{music}})t + \chi_i\right) \right\}, \tag{57}$$

which is formally identical to Eq. 55 but modulated by cross-modal coupling terms that broaden χ_i. Despite this, the net coherence remains higher than in the no-music case, leading to measurable enhancement in occipital alpha relative to ordinary eyes-open states, as has been observed in studies of meditative auditory processing [30].

Comparing the two conditions with and without music, the path integral model predicts that music amplifies auditory phase locking and strengthens cross-frequency coupling between auditory theta and occipital alpha. Without music, auditory cortex remains in a

low-amplitude idling state. With music, cross-modal integration results in measurable increases in coherence across auditory, occipital, and sensorimotor regions. This is further stabilized by body stillness, which maintains sensorimotor rhythm (SMR) c

$$\mathcal{Z}_{\text{music}} = \int \mathcal{D}[\phi(x,t)] \exp\left(\frac{i}{\hbar_B}\int dt\, d^3x\, \left[\mathcal{L}_{\text{auditory}} + \eta\phi(x,t)\cos(\omega_{\text{music}}t)\right]\right), \tag{58}$$

where η quantifies the strength of music-driven entrainment through mechanosensory and auditory pathways.

The measurable predictions are therefore clear. Meditation with music, eyes closed, produces enhanced theta and gamma coherence in auditory cortex and strong occipital alpha. Meditation with music, eyes open, produces persistent auditory phase locking with partial restoration of occipital alpha otherwise suppressed by visual inflow. Without music, auditory cortex shows only low-amplitude idling oscillations, and occipital alpha follows the usual eyes-open versus eyes-closed dynamics. These predictions can b

13 Emotional States in Meditation: Thalamus, Amygdala, and Limbic Dynamics

Meditative practice often progresses through stages of emotional depth, ranging from deep peace to serenity, bliss, and experiences described as universal love. These emotional states can be modeled within the path integral neurodynamics framework as emergent patterns of coherence across limbic, thalamic, and cortical structures. Each brain region contributes path amplitudes that evolve according to local Lagrangians, and the resulting global field arises as a coherent sum. In this section, we examine th The path integral representation of the emotional field is expressed as

$$\mathcal{A}_r(t) = \int \mathcal{D}[x_r(t)] \exp\left(\frac{i}{\hbar_B} S_r[x_r(t)]\right), \tag{59}$$

where r indexes regions such as the thalamus, amygdala, hippocampus, insula, cingulate cortex, and prefrontal cortex. The total emotional field is then defined as

$$\Phi_{\text{emotion}}(t) = \Re\left\{\sum_r \mathcal{A}_r(t)\right\}, \tag{60}$$

with the observed emotional state corresponding to the degree of coherence and phase alignment among the contributing amplitudes.

During the state of deep peace, the thalamus acts as a central hub for cortico-thalamic loops generating alpha and theta rhythms. In this state, the action functional $S_r[x_r(t)]$ for the thalamus is dominated by low-frequency oscillations, which synchronize with occipital alpha. The effective amplitude is expressed as

$$\mathcal{A}_{\text{thal}}(t) \sim E\exp(i\omega_\alpha t + \delta), \tag{61}$$

where ω_α corresponds to 8–12 Hz oscillations and δ a phase offset. The global emotional field becomes dominated by alpha coherence,

$$\Phi_{\text{peace}}(t) \approx \bar{E}\cos(\omega_\alpha t + \bar{\delta}), \tag{62}$$

predicting strong alpha power in EEG, consistent with reports of alpha enhancement during meditation associated with calm and peace [28].

In the state of serenity, limbic theta oscillations emerge with greater prominence. The hippocampus and anterior cingulate cortex generate theta rhythms in the range 4–7 Hz. The amplitude is represented as

$$\mathcal{A}_{\text{hip}}(t) \sim F\exp(i\omega_\theta t + \gamma), \tag{63}$$

where ω_θ is the theta frequency. The summation across hippocampal and frontal midline contributions yields

$$\Phi_{\text{serenity}}(t) \approx \bar{F}\cos(\omega_\theta t + \bar{\gamma}), \tag{64}$$

which manifests as frontal midline theta (Fmθ) in EEG recordings. This marker has been repeatedly associated with meditative serenity and internalized attention [30].

Blissful states are characterized by the coexistence of limbic theta with high-frequency gamma oscillations. The amygdala, hippocampus, and insula contribute to phase-amplitude coupling between theta and gamma. This can be modeled as

$$\mathcal{A}_{\text{bliss}}(t) \sim G\exp(i\omega_\theta t)\left[1 + \lambda\cos(\omega_\gamma t)\right], \tag{65}$$

where $\omega_\gamma > 2\pi \cdot 60$ rad/s and λ denotes the coupling strength. The resulting field

$$\Phi_{\text{bliss}}(t) \approx \bar{G}\cos(\omega_\theta t) + \lambda\bar{G}\cos(\omega_\theta t)\cos(\omega_\gamma t), \tag{66}$$

represents theta-modulated gamma bursts, which have been observed in advanced meditation practitioners reporting blissful experiences [31].

The state of universal love requires integration across limbic regions, thalamus, and prefrontal cortex. Here, the emotional field is described by a multi-frequency coherence function,

$$\Phi_{\text{love}}(t) = \sum_{r\in\{\text{limbic, thalamus, PFC}\}} K_r\cos(\omega_\theta t + \phi_r) + L_r\cos(\omega_\gamma t + \phi_r), \tag{67}$$

which emphasizes simultaneous theta and gamma synchrony across distributed networks. The prediction is widespread gamma coherence, cross-frequency coupling with theta, and high connectivity between prefrontal cortex and limbic structures. This corresponds to whole-brain integration, a phenomenon measurable with EEG coherence and phase-locking metrics.

The progression from peace to serenity, bliss, and universal love can also be modeled temporally as the narrowing of the distribution of neuronal trajectories in the functional integral. Initially, the spectral density $\rho(\omega)$ is broad, but with sustained meditation it contracts around dominant frequencies, allowing constructive interference. This process unfolds gradually over minutes, reflecting the time required to stabilize neuronal ensembles in the desired phase alignment. The convergence tim These predictions can be tested empirically using multimodal measures. EEG recordings should reveal increased alpha during peace,

frontal theta during serenity, theta-gamma coupling during bliss, and global gamma coherence during universal love. Functional MRI should reveal reduced amygdala activity, increased connectivity between prefrontal cortex and limbic regions, and thalamic regulation of cortical oscillations. Physiological correlates such as increased heart rate variability are also expected in

14 Measuring Deep Brain Structures in Meditation: fMRI, EEG, and Path Integral Integration

The study of meditation requires an understanding of not only cortical surface oscillations measurable with electroencephalography (EEG) but also of deeper brain structures such as the thalamus, amygdala, hippocampus, and broader limbic system. These regions are central to emotional regulation and consciousness, and their involvement has been highlighted in both neuroimaging and electrophysiological studies. Within the path integral formulation of neuronal dynamics, the amplitudes of these regions con Functional magnetic resonance imaging (fMRI) remains the principal noninvasive method for probing deep brain structures. fMRI measures blood-oxygen-level-dependent (BOLD) signals, which are indirect correlates of neural activity through neurovascular coupling. In the path integral context, the fMRI BOLD response can be modeled as the squared magnitude of the regional amplitude $\mathcal{A}_r(t)$ averaged over time:

$$\mathrm{BOLD}_r(t) \propto |\mathcal{A}_r(t)|^2 = \left| \int \mathcal{D}[x_r(t)] \exp\left(\frac{i}{\hbar_B} S_r[x_r(t)]\right) \right|^2, \tag{68}$$

where r denotes the region of interest. This relationship highlights that fMRI captures an integrated measure of neural coherence within a region rather than instantaneous phase information. Studies have shown reduced amygdala activation during meditation associated with emotional regulation [30], and enhanced thalamo-cortical coupling correlated with alpha oscillations reflecting states of peace [28].

EEG and magnetoencephalography (MEG) provide complementary temporal resolution, capturing oscillations in the millisecond range. While EEG is primarily sensitive to cortical surface activity, source reconstruction techniques such as sLORETA and beamforming allow estimation of deep sources including thalamus and hippocampus. The theoretical correspondence is given by

$$\Phi_{\mathrm{EEG}}(t) = \Re\left\{ \sum_r W_r \mathcal{A}_r(t) \right\}, \tag{69}$$

where W_r represents the projection weight of region r onto the scalp electrodes. MEG, due to its sensitivity to magnetic fields, can detect synchronous currents in deeper regions with better spatial resolution than EEG, though still subject to inverse modeling constraints.

The thalamus, acting as a relay hub, generates rhythms in the alpha and theta range. Its contribution to the global field during meditation can be written as

$$\mathcal{A}_{\mathrm{thal}}(t) \sim H \exp(i\omega_\alpha t + \phi_{\mathrm{thal}}), \tag{70}$$

where ω_α is the alpha frequency and ϕ_{thal} the thalamic phase. This aligns with fMRI studies showing thalamic involvement in meditative states characterized by deep peace. The amygdala, central to emotional salience, exhibits decreased BOLD amplitude during serenity, which may be modeled as a reduction in amplitude coefficients $|\mathcal{A}_{\text{amyg}}(t)|$.

The hippocampus and limbic system are critical for the transition to bliss and universal love. These states are associated with theta-gamma coupling, which in fMRI appears as rhythmic modulation of BOLD signals in the hippocampus and anterior cingulate cortex. The path integral representation is given by

$$\mathcal{A}_{\text{hip}}(t) \sim J \exp(i\omega_\theta t) \left[1 + \lambda \cos(\omega_\gamma t)\right], \tag{71}$$

producing measurable theta-gamma phase-amplitude coupling in EEG and corresponding BOLD fluctuations in fMRI. This dual-measurement paradigm allows both temporal and spatial characterization of deep limbic involvement.

Prefrontal cortex (PFC) integration with limbic regions during universal love is reflected in increased functional connectivity, observable in fMRI as correlated BOLD fluctuations between PFC and hippocampus, and in EEG/MEG as global gamma synchrony. The functional connectivity in fMRI is mathematically related to the correlation of squared amplitudes,

$$\text{FC}_{\text{PFC-limbic}} = \langle \text{BOLD}_{\text{PFC}}(t)\, \text{BOLD}_{\text{limbic}}(t) \rangle, \tag{72}$$

while the EEG equivalent is coherence in the gamma band,

$$C_\gamma(f) = \frac{|\langle \Phi_{\text{PFC}}(f) \Phi^*_{\text{limbic}}(f) \rangle|}{\sqrt{\langle |\Phi_{\text{PFC}}(f)|^2 \rangle \langle |\Phi_{\text{limbic}}(f)|^2 \rangle}}, \tag{73}$$

where $\Phi(f)$ are Fourier transforms of regional fields. This illustrates the complementarity of fMRI and EEG/MEG in mapping deep emotional states during meditation.

Invasive recordings, such as stereo-EEG or deep brain stimulation electrodes, offer direct measurements of amygdala, hippocampus, and thalamus activity, though such methods are limited to clinical contexts. These recordings confirm the oscillatory dynamics inferred from noninvasive methods, providing a bridge between human meditation studies and direct neuronal measures.

In conclusion, deep brain structures essential for meditation can be measured effectively using fMRI for spatial localization, EEG and MEG for temporal coherence, and combined methods for integration within the path integral framework. Predictions include enhanced thalamic alpha coherence during deep peace, reduced amygdala amplitude during serenity, hippocampal theta-gamma coupling during bliss, and widespread PFC-limbic connectivity during universal love. These predictions are measurable with combined f

15 Prefrontal Cortex Dynamics and EEG Changes During Meditation

The prefrontal cortex (PFC) plays a central role in meditation, acting as a hub for attentional regulation, executive control, and emotional modulation. Within the path integral

framework of brain dynamics, the neuronal ensembles of the PFC contribute amplitudes that evolve according to the local action functional, and their degree of coherence determines the observable electroencephalographic (EEG) signals. Meditation induces specific changes in the spectral composition and coherence of PFC oscillation One of the most robust markers of meditation in the PFC is the increase in frontal midline theta activity, typically in the 4–7 Hz range. This rhythm reflects focused attention, internalized monitoring, and cognitive control. The neuronal amplitude of a single PFC oscillator contributing to theta activity may be expressed as

$$\mathcal{A}_{\mathrm{PFC},\theta}(t) \sim A_\theta \exp(i\omega_\theta t + \phi_\theta), \tag{74}$$

where $\omega_\theta \approx 2\pi \cdot 6$ rad/s. The macroscopic field emerging from the summation across PFC neurons is then

$$\Phi_{\mathrm{PFC},\theta}(t) = \Re\left\{ \sum_{i \in \Omega_{\mathrm{PFC}}} \mathcal{A}_{i,\theta}(t) \right\}. \tag{75}$$

During meditation, phase dispersion among oscillators in Ω_{PFC} is reduced, producing constructive interference and yielding a stable frontal midline theta field. This corresponds to the frontal midline theta observed in EEG studies of meditation [30].

Alongside theta, the PFC exhibits increased alpha oscillations in the 8–12 Hz band during meditation. Alpha rhythms in the PFC reflect inhibitory control over irrelevant processing and contribute to the state of relaxed alertness characteristic of meditative practice. A typical neuronal amplitude in this case is given by

$$\mathcal{A}_{\mathrm{PFC},\alpha}(t) \sim A_\alpha \exp(i\omega_\alpha t + \phi_\alpha), \tag{76}$$

with $\omega_\alpha \approx 2\pi \cdot 10$ rad/s. The macroscopic alpha field in the PFC is then

$$\Phi_{\mathrm{PFC},\alpha}(t) = \Re\left\{ \sum_{i \in \Omega_{\mathrm{PFC}}} \mathcal{A}_{i,\alpha}(t) \right\}, \tag{77}$$

which gains coherence during meditation as neuronal ensembles align their phases. Increased frontal alpha during meditation has been reported in empirical EEG studies, reflecting a reduction in discursive thought and heightened attentional control [32].

A hallmark of advanced meditative states is the emergence of high-amplitude gamma synchrony in the PFC, often exceeding 30 Hz and extending above 60 Hz. Gamma oscillations in the PFC indicate large-scale binding of cognitive and affective processes and have been especially associated with compassion and loving-kindness practices. The amplitude of a PFC oscillator contributing to gamma activity can be written as

$$\mathcal{A}_{\mathrm{PFC},\gamma}(t) \sim A_\gamma \exp(i\omega_\gamma t + \phi_\gamma), \tag{78}$$

where ω_γ lies in the gamma band. The interaction of theta and gamma rhythms can be captured through a phase-amplitude coupling representation,

$$\mathcal{A}_{\mathrm{PFC}}(t) \sim A_\theta \exp(i\omega_\theta t)\left[1 + \lambda \cos(\omega_\gamma t)\right], \tag{79}$$

where λ is the coupling strength. This model predicts theta-modulated gamma bursts in the PFC, a phenomenon observed in EEG recordings of advanced meditators [31].

Beta activity in the range 13–30 Hz, often associated with habitual and discursive cognitive processing, tends to decrease during meditation. This reduction can be expressed as a relative decrease in amplitude coefficients,

$$|\mathcal{A}_{\mathrm{PFC},\beta}(t)|^2 \downarrow, \tag{80}$$

indicating that the action functional governing PFC oscillations during meditation suppresses beta contributions while enhancing theta, alpha, and gamma coherence.

The overall PFC field during meditation may therefore be represented as a coherent superposition of these components,

$$\Phi_{\mathrm{PFC}}(t) = \Phi_{\mathrm{PFC},\theta}(t) + \Phi_{\mathrm{PFC},\alpha}(t) + \Phi_{\mathrm{PFC},\gamma}(t), \tag{81}$$

with the relative weights of each rhythm evolving as meditation deepens. Early stages are dominated by theta, intermediate stages show stronger alpha, and advanced states feature gamma synchrony nested within slower oscillations. The reduction of beta further reinforces the dominance of rhythms associated with meditative absorption.

These predictions are supported by neurophysiological evidence. Increased frontal midline theta has been associated with meditative focus and emotional regulation [30]. Enhanced prefrontal alpha has been reported in mindfulness studies, where it correlates with improved attentional control and reduced self-referential activity [32]. High-amplitude gamma synchrony in the PFC has been observed in long-term meditators practicing compassion meditation [31]. Together, t Within the path integral formulation, meditation progressively narrows the distribution of trajectories $x_i(t)$ in the PFC action functional $S_{\mathrm{PFC}}[x]$, leading to increasing coherence of neuronal amplitudes. The PFC thereby serves as a critical node in the emergence of meditative states, integrating cognitive control, affect regulation, and inter-regional synchrony. The EEG correlates of this process provide measurable evidence for the theoretical model, offering a bridge between the quantitat

16 Conclusion

In this work we have advanced a unified theoretical framework linking electroencephalography (EEG), path integral formulations of neuronal activity, and mechanosensitive modulation through Piezo2 ion channels. Neurons were modeled as mesoscopic quantum oscillators governed by a brain-specific Planck-like constant h_{Neuron}, enabling the use of path integral methods to represent neuronal trajectories and their superposition into emergent macroscopic fields. Within this framework, EEG rhythms arise from t The integration of Piezo2-driven vascular modulation highlights the role of neurovascular dynamics in shaping neuronal coherence. By coupling fast hemodynamic oscillations to cortical rhythms, Piezo2 channels provide a biophysical mechanism for entraining neuronal ensembles, thereby influencing EEG patterns. This represents a bridge between microscopic neuronal path integrals and macroscopic physiological rhythms of the brain and body.

Meditative practice provided a valuable domain in which to test these ideas. Predictions were developed for sensorimotor rhythm stabilization during bodily stillness, occipital alpha modulation during eyes-open and eyes-closed states, auditory cortex entrainment in

response to music, and prefrontal cortex shifts from theta to gamma dominance across meditative depth. Emotional states such as peace, serenity, bliss, and universal love were interpreted in terms of thalamo-cortical and limbic-prefrontal coh The conclusions of this study are twofold. First, EEG can be rigorously interpreted as the macroscopic manifestation of neuronal path integrals modulated by mechanosensory inputs, providing a theoretical foundation that unites electrophysiology, neuroimaging, and quantum-inspired models of brain function. Second, meditation serves as an experimental paradigm where theoretical predictions can be tested against empirical data, offering a bridge between subjective experience and measurable neurophysiology.

Future research directions include experimental quantification of the brain-specific Planck constant h_{Neuron}, validation of Piezo2-mediated neurovascular coupling in meditation, and multimodal integration of EEG, MEG, and fMRI to probe deep brain structures within the path integral framework. By combining theory and experiment, the approach developed here aspires to contribute toward a comprehensive scientific account of consciousness grounded in measurable neuronal and systemic processes.

References

[1] J.C. Eccles and F. Beck, Quantum Aspects of Brain Activity and the Role of Consciousness, *Proc. Natl. Acad. Sci.* (1992).

[2] J.C. Eccles and K. Popper, *The Self and Its Brain*, Springer, Berlin (1977).

[3] F. Crick, *The Astonishing Hypothesis*, Simon and Schuster (1994).

[4] A. Eddington, *The Nature of the Physical World*, (1928).

[5] N. Bohr, *Atomic Physics and Human Knowledge*, (1958).

[6] W. Heisenberg, *Über den anschaulichen Inhalt der quantentheoretischen Kinematik und Mechanik*, Z. Phys. (1927).

[7] E.P. Wigner, *Remarks on the Mind-Body Question*, in Symmetries and Reflections (1967).

[8] J.A. Wheeler, *Law Without Law*, in Quantum Theory and Measurement (1983).

[9] R. Penrose and C. J. Isham, *Quantum Concepts in Space Time*, Oxford Univ. Press (1986).

[10] J. von Neumann, *Mathematical Foundations of Quantum Mechanics*, Princeton Univ. Press (1955).

[11] M.S. Modgil, Axioms for a Differential Geometric Approach to von Neumann's Theory of Quantum Measurement, *Int. J. Quantum Foundations* (2024).

[12] Y. Zhao, Y. Lian, H. Di, and W. Zhao, "Rapid coupling between vasculature and neurons through mechanosensitive channels in the olfactory lobe," *Frontiers in Human Neuroscience*, vol. 18, 2024. doi:10.3389/fnhum.2024.1435859.

[13] L. Jammal Salameh et al., "Blood pressure pulsations modulate central neuronal activity via mechanosensitive ion channels," *Science*, vol. 383, 2024. doi:10.1126/science.adk8511.

[14] S. Chi et al., "Astrocytic Piezo1-mediated mechanotransduction determines adult neurogenesis and cognitive functions," *Neuron*, vol. 110, pp. 2984–2999.e8, 2022. doi:10.1016/j.neuron.2022.07.010.

[15] J. C. Eccles and F. Beck, "Quantum aspects of brain activity and the role of consciousness," *Proc. Natl. Acad. Sci.*, vol. 89, no. 16, pp. 7320–7324, 1992.

[16] E. P. Wigner, "Remarks on the mind-body question," in *Symmetries and Reflections*, Indiana Univ. Press, 1967.

[17] M. S. Modgil, "Quantum Potential and Neuron's Firing: Bohmian Neurodynamics," arXiv preprint arXiv:2504.0051, 2025.

[18] D. Bohm and B. J. Hiley, *The Undivided Universe: An Ontological Interpretation of Quantum Theory*, Routledge, 1993.

[19] J. C. Eccles and F. Beck, "Quantum aspects of brain activity and the role of consciousness," *Proc. Natl. Acad. Sci.*, vol. 89, pp. 7320–7324, 1992

[20] M. S. Modgil, "Path Integral Formulation of the Quantum Brain: Neurons as Quantum Mechanical Oscillator," arXiv preprint arXiv:2504.0051v1, 2025.

[21] R. P. Feynman and A. R. Hibbs, *Quantum Mechanics and Path Integrals*, McGraw-Hill, 1965.

[22] O. P. Hamill and B. Martinac, "Molecular basis of mechanotransduction in Piezo channels," *Annual Review of Physiology*, vol. 83, pp. 431–453, 2021.

[23] G. Buzsáki, *Rhythms of the Brain*, Oxford University Press, 2006.

[24] M. B. Sterman, "Physiological origins and functional correlates of EEG rhythmic activities: implications for self-regulation," *Biofeedback and Self-regulation*, vol. 21, no. 1, pp. 3–33, 1996.

[25] G. Pfurtscheller and F. H. Lopes da Silva, "Event-related EEG/MEG synchronization and desynchronization: basic principles," *Clinical Neurophysiology*, vol. 110, pp. 1842–1857, 1999.

[26] H. Berger, "Über das Elektrenkephalogramm des Menschen," *Archiv für Psychiatrie und Nervenkrankheiten*, vol. 87, pp. 527–570, 1929.

[27] G. Pfurtscheller and F. H. Lopes da Silva, "Event-related EEG/MEG synchronization and desynchronization: basic principles," *Clinical Neurophysiology*, vol. 110, no. 11, pp. 1842–1857, 1999.

[28] F. H. Lopes da Silva, "Neural mechanisms underlying brain waves: from neural membranes to networks," *Electroencephalography and Clinical Neurophysiology*, vol. 79, no. 2, pp. 81–93, 1991.

[29] M. B. Sterman, "Physiological origins and functional correlates of EEG rhythmic activities: implications for self-regulation," *Biofeedback and Self-regulation*, vol. 21, no. 1, pp. 3–33, 1996.

[30] L. I. Aftanas and S. A. Golocheikine, "Human anterior and frontal midline theta and lower alpha reflect emotionally positive state and internalized attention: high-resolution EEG investigation of meditation," *Neuroscience Letters*, vol. 310, no. 1, pp. 57–60, 2001.

[31] A. Lutz, L. L. Greischar, N. B. Rawlings, M. Ricard, and R. J. Davidson, "Long-term meditators self-induce high-amplitude gamma synchrony during mental practice," *Proceedings of the National Academy of Sciences*, vol. 101, no. 46, pp. 16369–16373, 2004.

[32] T. Lomas, M. Ivtzan, and D. Fu, "A systematic review of the neurophysiology of mindfulness on EEG oscillations," *Neuroscience & Biobehavioral Reviews*, vol. 57, pp. 401–410, 2015.

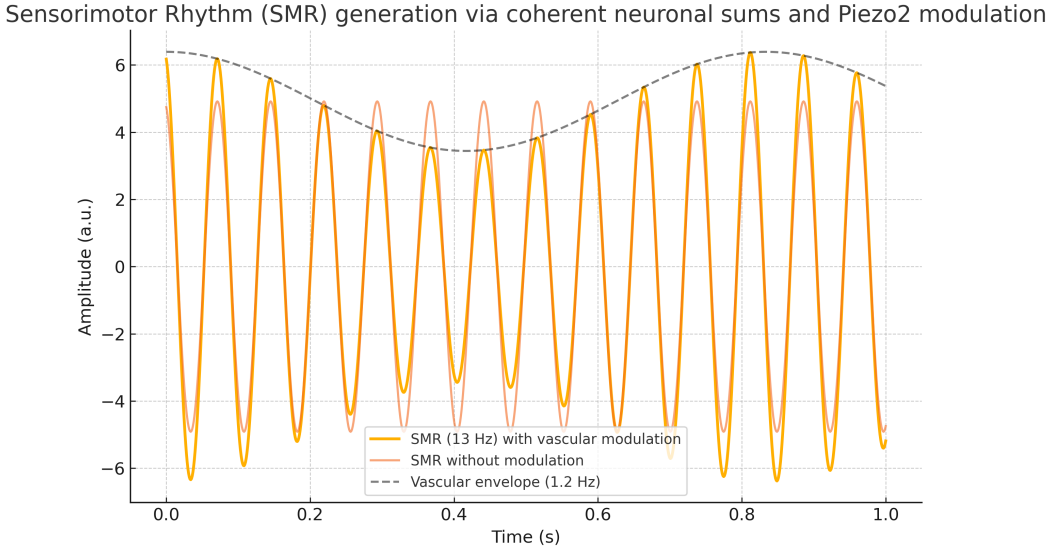

Figure 1: Illustration of Sensorimotor Rhythm (SMR) generation as a coherent sum over neuronal oscillations at ∼13 Hz, modulated by Piezo2-driven vascular pulsations (∼1.2 Hz). The black dashed line shows the vascular envelope, the blue curve shows SMR without modulation, and the red curve shows the modulated SMR field observable in EEG.

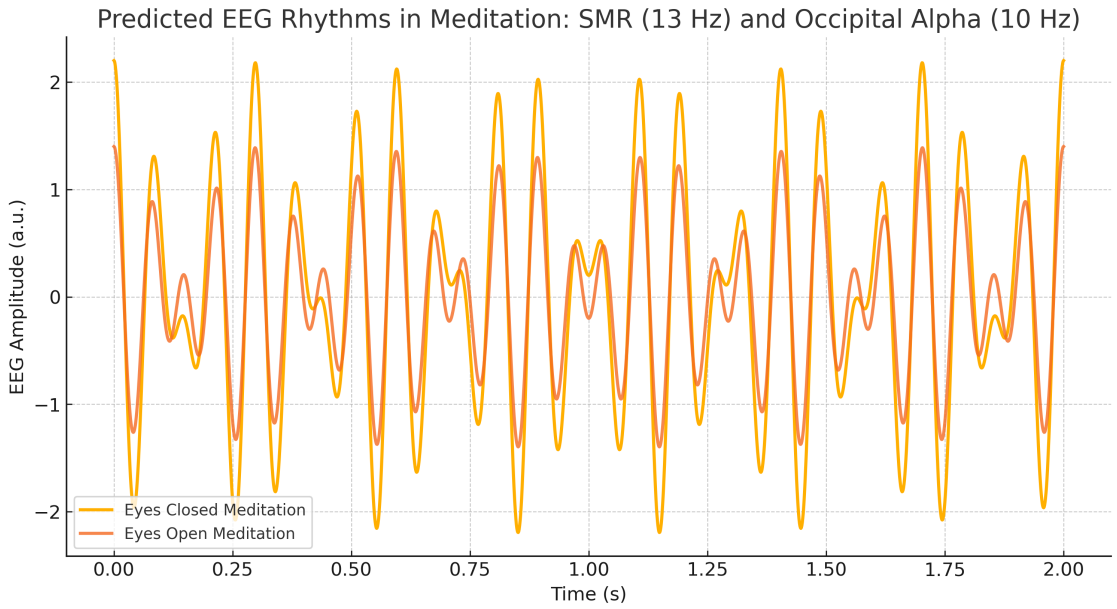

Figure 2: Predicted EEG rhythms during meditation. With eyes closed (blue), both SMR (∼13 Hz) and occipital alpha (∼10 Hz) show strong coherence due to constructive interference across neuronal ensembles. With eyes open (orange), SMR remains moderate while occipital alpha, normally suppressed, re-emerges with partial coherence due to attentional regulation in meditative focus.

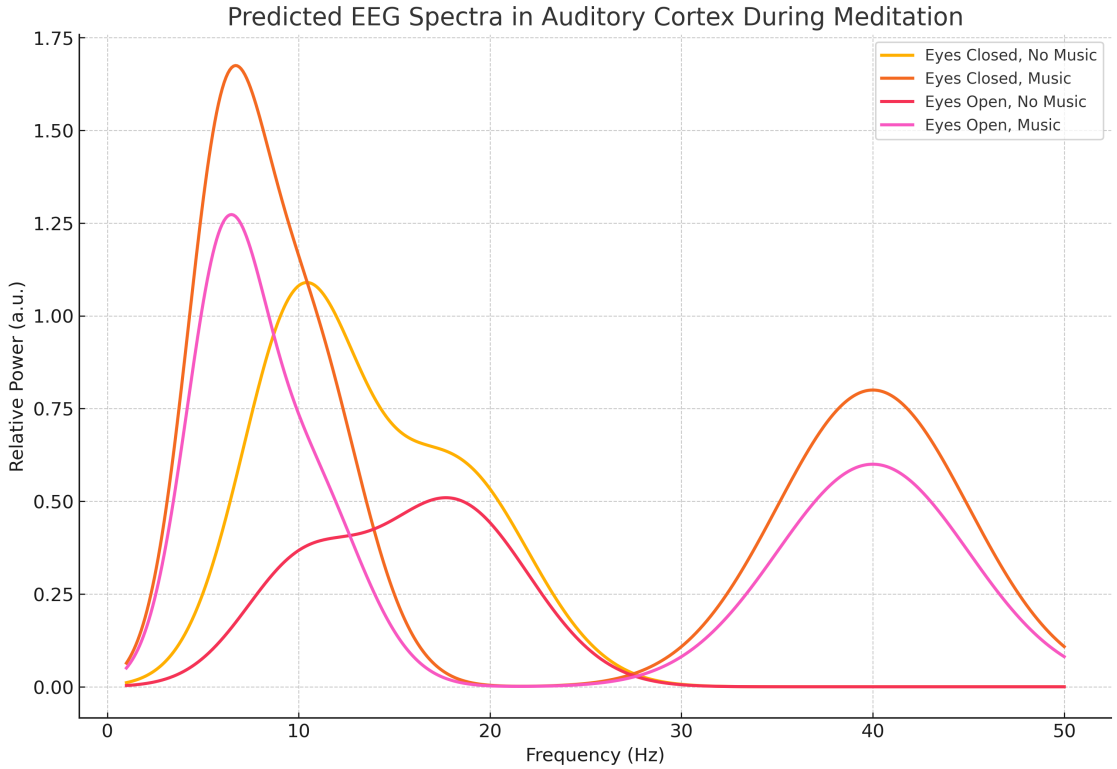

Figure 3: Predicted EEG spectra in the auditory cortex during meditation under four conditions. (1) Eyes closed, no music: idling rhythms with alpha peak. (2) Eyes closed, music: entrainment produces strong theta and gamma peaks alongside alpha. (3) Eyes open, no music: occipital alpha suppressed, auditory cortex shows weak activity. (4) Eyes open, music: entrainment stabilizes coherence, restoring partial alpha and enhancing theta/gamma.

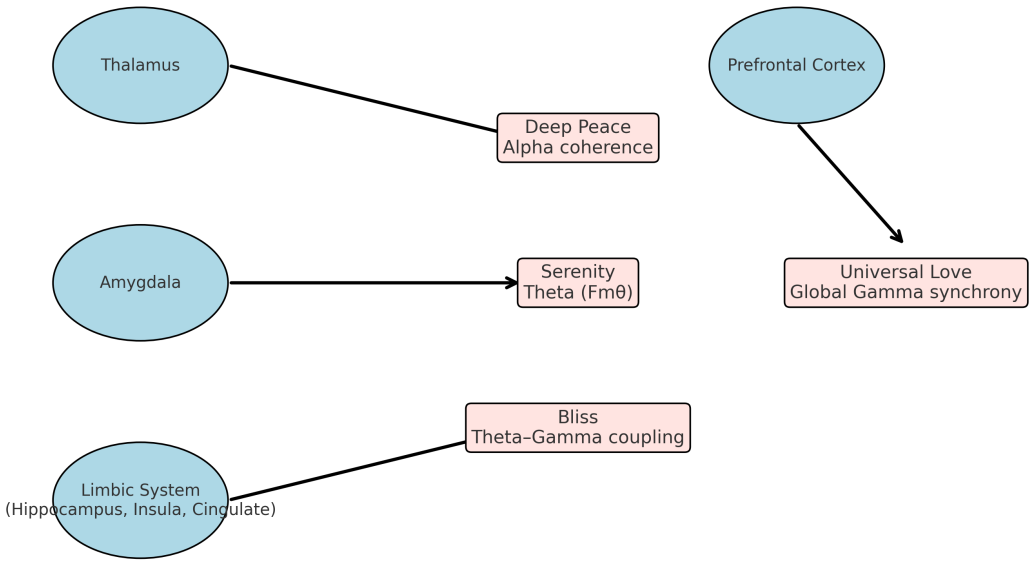

Figure 4: Progression of emotional states during meditation. The thalamus supports alpha coherence associated with deep peace. The amygdala and limbic theta activity contribute to serenity. Bliss emerges from theta–gamma coupling in the limbic system. Universal love involves global gamma synchrony integrating prefrontal cortex, limbic structures, and thalamus.

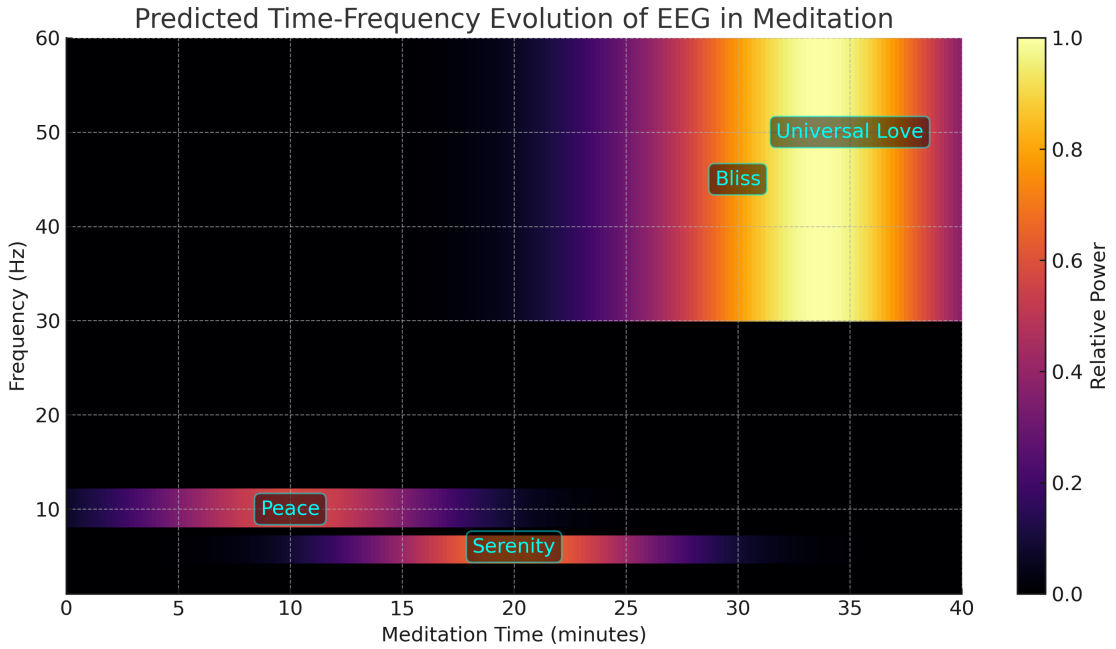

Figure 5: Predicted time-frequency evolution of EEG rhythms during meditation. Early meditation (around 10 minutes) is dominated by alpha (8–12 Hz) associated with deep peace. Mid meditation (around 20 minutes) shows increased frontal theta (4–7 Hz) corresponding to serenity. Later stages (30 minutes) display theta-modulated gamma bursts (>30 Hz) linked with bliss. Finally, widespread gamma synchrony (35 minutes onward) reflects the state described as universal love.

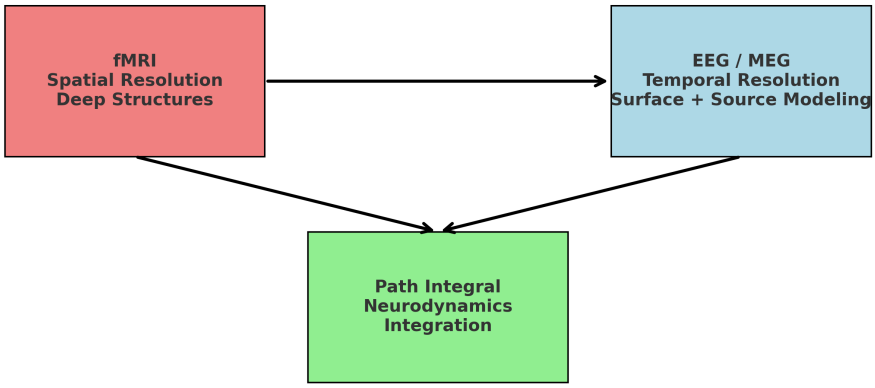

Figure 6: Integration of measurement modalities. fMRI provides spatial resolution of deep brain structures such as thalamus, amygdala, and hippocampus, while EEG/MEG provide high temporal resolution of oscillatory dynamics, with partial access to deep structures through source modeling. The path integral neurodynamics framework integrates these complementary measurements into a unified model of meditation states.

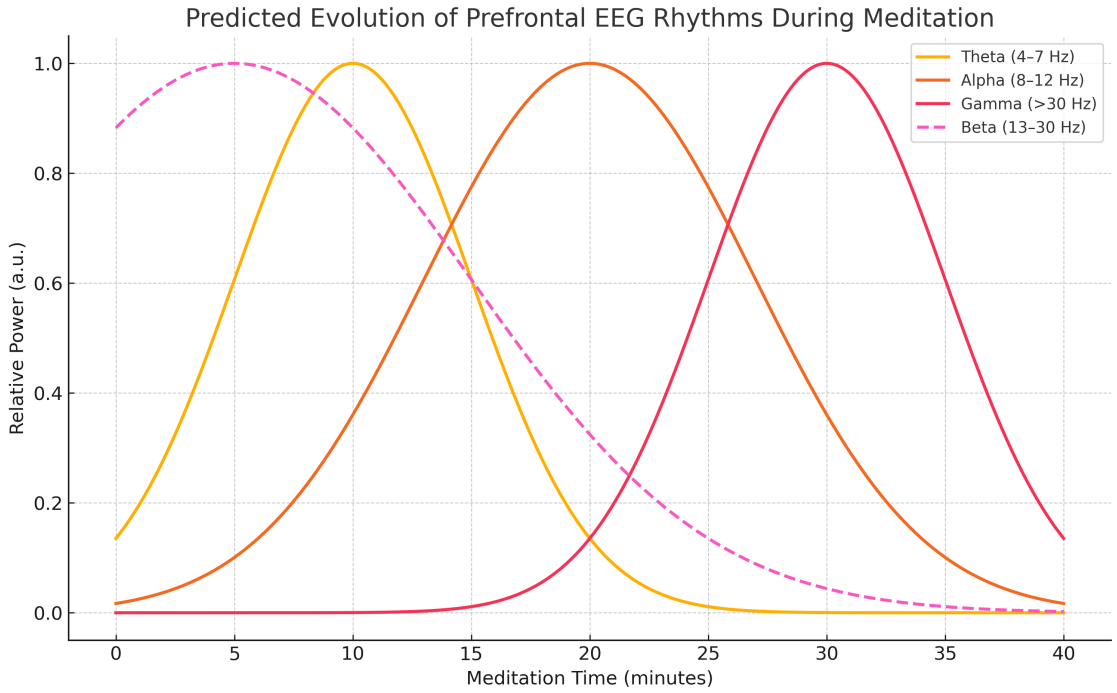

Figure 7: Predicted evolution of prefrontal EEG rhythms during meditation. Theta (4–7 Hz) rises in early stages, reflecting focused attention. Alpha (8–12 Hz) emerges in intermediate stages, associated with relaxed alertness. Gamma activity (>30 Hz) dominates in advanced stages, linked with integrative states such as compassion and universal love. Beta (13–30 Hz), associated with discursive thought, decreases as meditation deepens.

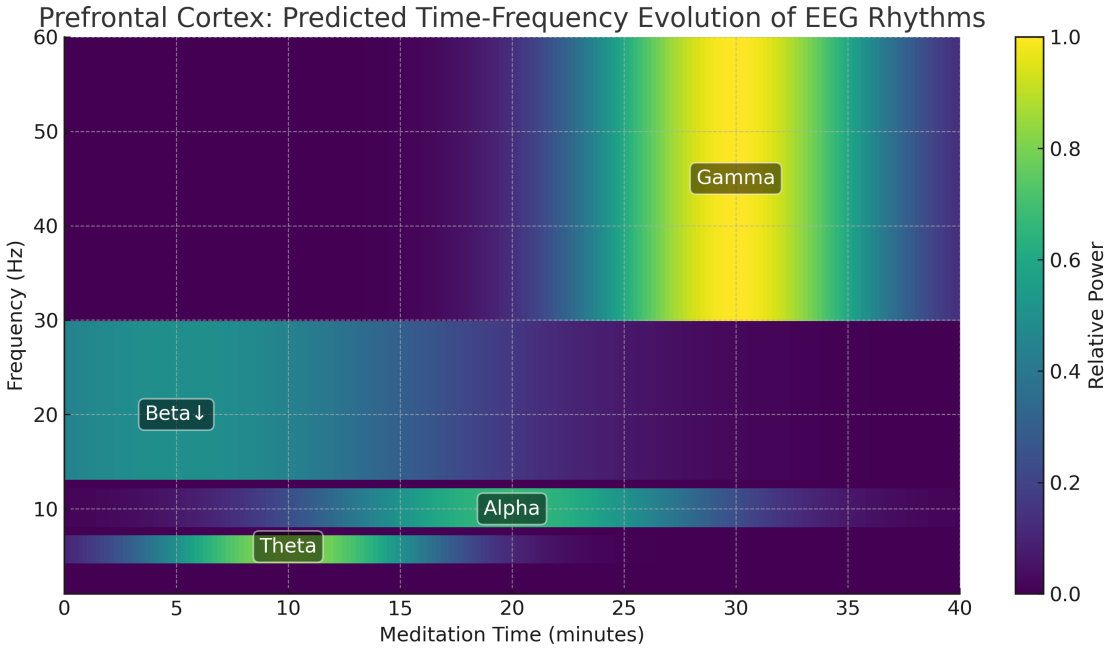

Figure 8: Predicted time-frequency evolution of prefrontal cortex EEG rhythms during meditation. Early stages show increased theta (4–7 Hz), mid stages show rising alpha (8–12 Hz), advanced stages show strong gamma activity (>30 Hz), and beta activity (13–30 Hz) decreases as meditation progresses. This dynamic progression reflects the prefrontal cortex's role in focused attention, relaxed alertness, and higher integrative states.